Supplementary Appendix

This appendix has been provided by the authors to give readers additional information about their work.

Supplement to: Shaw AT, Friboulet L, Leshchiner I, et al. Resensitization to crizotinib by the lorlatinib *ALK* resistance mutation L1198F. N Engl J Med 2016;374:54-61. DOI: 10.1056/NEJMoa1508887

SUPPLEMENTARY APPENDIX

Supplement to: Shaw et al. Resistance to the Next Generation ALK Inhibitor Lorlatinib Restores Sensitivity to Crizotinib

Contents **Page**

Supplementary Methods 2
Figure S1. Identification of ALK C1156Y/L1198F by Sanger Sequencing 7
Figure S2. Phylogenetic Relationship of Pre-Treatment and Resistant Samples 8
Figure S3. Suppression of ALK C1156Y/L1198F Phosphorylation by Crizotinib 9
Figure S4. Resensitization of Crizotinib-Resistant ALK Mutants by L1198F 10
Figure S5. Co-crystal Structures of ALK C1156Y with Crizotinib 11
Figure S6. Co-crystal Structures of ALK C1156Y and C1156Y/L1198F with Crizotinib or Lorlatinib 12
Table S1. Cell Survival Assays in Ba/F3 Models of ALK Resistance 13
Table S2. Cell Survival Assays in Ba/F3 Models Expressing Different ALK L1198F Mutants 14
Table S3. Inhibition Constants of ALK Inhibitors with Wildtype and Mutant ALK Kinase Domains 15
Table S4. Kinetic Parameters of Wildtype and Mutant ALK Kinase Domains 16
Table S5. Computational Models Comparing Wildtype ALK and ALK L1198F Binding to Crizotinib and Lorlatinib 17
Table S6. Energetics of Crizotinib and Lorlatinib Binding to Wildtype and Mutant ALK Kinase Domains 18
References 19

SUPPLEMENTARY METHODS

Isolation and Sequencing of Nucleic Acid

For snapshot-NGS analysis (v1.1.4), genomic DNA was isolated from formalin-fixed paraffin embedded (FFPE) tumor specimens. The DNA was sheared with the Covaris M220 instrument, followed by end repair, adenylation, and ligation with an adapter. A sequencing library targeting hotspots and exons in 39 genes was generated using two hemi-nested PCR reactions. Illumina MiSeq 2 x 151 base paired-end sequencing results were aligned to the hg19 human genome reference using BWA-MEM[1]. MuTect[2] and a laboratory-developed insertion/deletion analysis algorithm were used for SNV and indel variant detection, respectively. This assay can detect SNV and indel variants at ≥5% allelic frequency in target regions with sufficient read coverage.

For Sanger sequencing of cDNA, RNA was isolated from flash frozen tumor specimens and cDNA was generated. EML4-ALK was amplified using primers 1F (TCCAGAAAGCAAGAATGCTACTCC) and 4193R (ggcaaagcggtgttgattacatcc). The entire ALK kinase domain was sequenced using the primers 3221F (agagccctgagtacaagctgag) and 4193R.

For whole exome sequencing, genomic DNA was extracted from FFPE tumor samples. Whole-exome capture libraries were constructed from 100ng of extracted tumor and normal DNA following shearing, end repair, phosphorylation and ligation to barcoded sequencing adapters[3,4]. Ligated DNA was size-selected for lengths between 200-350bp and subjected to exonic hybrid capture using SureSelect v2 Exome bait (Agilent). Samples were multiplexed and sequenced on multiple Illumina HiSeq flowcells (paired end 76bp reads) to average depth of coverage of 116-185x and 125x for tumor and normals, respectively.

Analysis of Whole Exome Sequencing

Massively parallel sequencing data were processed using two consecutive pipelines: (1) The sequencing data processing pipeline, called “Picard”, developed by the Sequencing Platform at the Broad Institute, starts with the reads and qualities produced by the Illumina software for all lanes and libraries generated for a single sample (either tumor or normal) and produces, at the end of the pipeline, a single BAM file (http://samtools.sourceforge.net/SAM1.pdf) representing the sample. (2) The Broad Cancer Genome Analysis pipeline, also known as “Firehose” (www.broadinstitute.org/cancer/cga/Firehose), starts with the BAM files for each sample and matched normal sample from peripheral blood (hg19), and performs various analyses, including quality control, local realignment, mutation calling, small insertion and deletion identification, rearrangement detection, coverage calculations and others. The details of our sequencing data processing have been described elsewhere[5,6] (see www.broadinstitute.org/cancer/cga). Somatic single-nucleotide variations (SSNVs) were detected using MuTect[2]. Single nucleotide variants found within coding areas of the genome were annotated for the chromosomal location, the type of the variant, the codon change and the change in the protein sequence using Oncotator[7]. Insertions and deletions in coding areas (both frameshift and in-frame) were detected using the algorithm Indelocator (www.broadinstitute.org/cancer/cga/Indelocator).

We used the ABSOLUTE algorithm to calculate the purity, ploidy, and absolute DNA copy-numbers of each sample[8]. Following the framework previously described[8], we computed the posterior probability distribution over CCF. Further details of this procedure were described recently[9].

Clustering analysis of SSNVs

We employed a previously described Bayesian clustering procedure[10]. The details of this procedure have been recently described[9,11]. This approach exploits the assumption that the observed subclonal SSNV CCF values were sampled from a smaller number of subclonal cell

populations (subclones). All remaining uncertainty (including the exact number of clusters) was integrated out using a mixture of Dirichlet processes, which was fit using a Gibbs sampling approach, building on a previously described framework[10].

Ba/F3 Cell Line Studies

Ba/F3 cells were engineered to express *EML4-ALK* harboring different ALK resistance mutations as previously described[12]. Cells were seeded in triplicate into 96-well plates and cultured overnight. Serial dilutions of different ALK inhibitors were added to the wells, and cells were incubated for 48 hours. Cell viability was determined using Cell Titer Glo (Promega). IC50 values were calculated by concentration-response curve fitting utilizing a four-parameter analytical method. Crizotinib, ceritinib, and brigatinib were purchased from Selleckchem. Alectinib was purchased from Active Biochem. Lorlatinib was provided by Pfizer.

Binding Affinities and Enzyme Kinetics

Recombinant human wildtype and mutant ALK kinase domain proteins (amino acids 1093-1411) were produced in house using baculoviral expression and pre-activated by autophosphorylation of 10-100 μM enzyme in 100 mM Hepes, pH 7.1, 20 mM $MgCl_2$, 4 mM ATP for 1-4 hours at room temperature to achieve maximal activity. ALK Ki inhibition constants were determined by a microfluidic mobility shift assay using 11 doses of 3-fold serially diluted inhibitors (0-1 μM) at 4 concentrations of ATP (0.25-2 mM) and global fitting initial reaction velocities to a Morrison equation for competitive inhibition as previously described[13,14]. The reactions contained 1, 0.2, 2.5 or 0.4 nM of wildtype, C1156Y, L1198F or C1156Y/L1198F mutant ALK enzyme, respectively. Kinetic parameters were determined by a coupled spectrophotometric ATP-regenerating assay as previously reported[15] using a “YFF” ALK activation loop peptide

(ARDIYRASFFRKGGCAMLPVK) as a phosphoacceptor substrate, which was reported to be phosphorylated more rapidly than the wild-type "YYY" peptide[16]. The reactions contained 10, 2.5, 25, or 5 nM of wildtype, C1156Y, L1198F or C1156Y/L1198F mutant ALK enzyme, respectively, and 7.8-500 μM YFF peptide and 1 mM ATP to generate $K_{M,YFF}$ or 7.8-1000 μM ATP and 1 mM YFF peptide to generate $K_{M,ATP}$. Reactions were started by adding ATP and conducted at 30 °C. Initial reaction velocities were fit to a Michalis-Menten equation using GraphPad Prism (GraphPad Software, San Diego, CA) to determine the turnover number, k_{cat}, and Michaelis constants, K_M, for ATP and YFF substrate.

Co-crystal Structures

The mutant ALK co-crystal structures with crizotinib or lorlatinib described here have been deposited to the Protein Data Bank (wwPDB) and the details of the methods used can be found under accession codes: 5A9U (C1156Y ALK+lorlatinib, 1.6 Å), 5AA8 (C1156Y/L1198F ALK+lorlatinib, 1.86 Å), 5AA9 (L1198F ALK+lorlatinib, 1.77 Å), 5AAA (L1198F ALK+crizotinib, 1.73 Å), 5AAB (C11156Y/L1198F ALK+crizotinib, 2.2 Å), and 5AAC (C1156Y ALK+crizotinib, 1.70 Å). Non-phosphorylated human mutant ALK kinase domain proteins (amino acids 1093-1411) were crystallized by the hanging drop vapor diffusion method at 13 °C by mixing 2 μL of purified protein solution (11-15 mg/mL) containing crizotinib or lorlatinib at a 2x stoichiometric ratio to protein with 2 μL of solutions containing 0.2 M lithium sulfate, 17-21% PEG MW=3350, and 0.1 M Tris pH range 7.6-8.5.

Isothermal Titration Calorimetry (ITC)

Binding experiments were carried out on a VP ITC instrument (Malvern Instruments) at 20 °C. Compound binding to nonphosphorylated ALK kinase domain proteins was measured in 150 mM NaCl, 25 mM HEPES, pH 7.5, 5 mM $MgCl_2$, 10% glycerol, 1 mM TCEP and 1% DMSO.

Data was analyzed using the ORIGIN software by 1:1 binding model except for lorlatinib which was analyzed using a displacement binding approach to extend the detection limit of the technique. Standard deviation was calculated from triplicate experiments.

Computational Binding Studies

Free-energy perturbation with replica exchange with solute tempering (FEP/REST; Schrodinger 2015-2; Desmond: FEP Protein Mutation for Ligand Selectivity; default settings; OPLS2.1 FF models). Protein Models: PDB 2XP2 crizotinib bound to ALK kinase domain protein. All missing loops were modeled using PRIME. Ligand Models: Published co-crystal structures were aligned to crizotinib-ALK co-crystal structure.

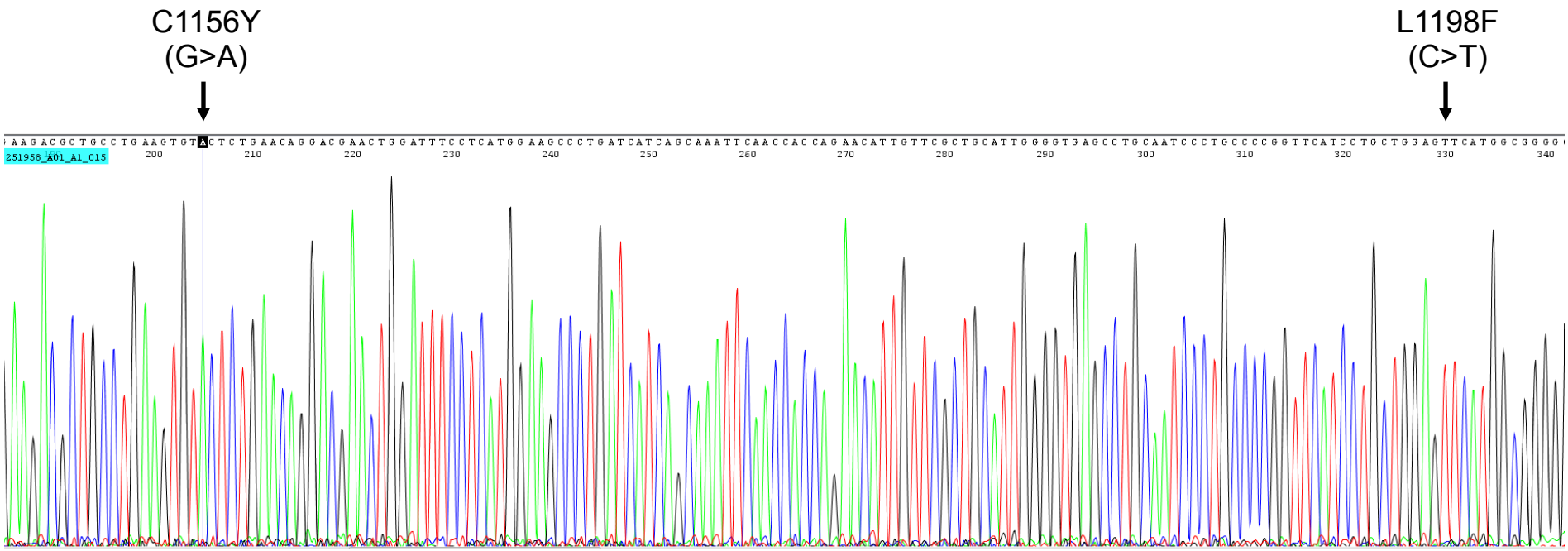

Figure S1. Identification of ALK C1156Y/L1198F by Sanger Sequencing
EML4-ALK was amplified from cDNA as described in the text. PCR products were subcloned into the pCR4-TOPO vector, and individual bacterial colonies were sequenced. Shown is a representative chromatogram demonstrating the presence of both ALK C1156Y and L1198F mutations in a single bacterial clone.

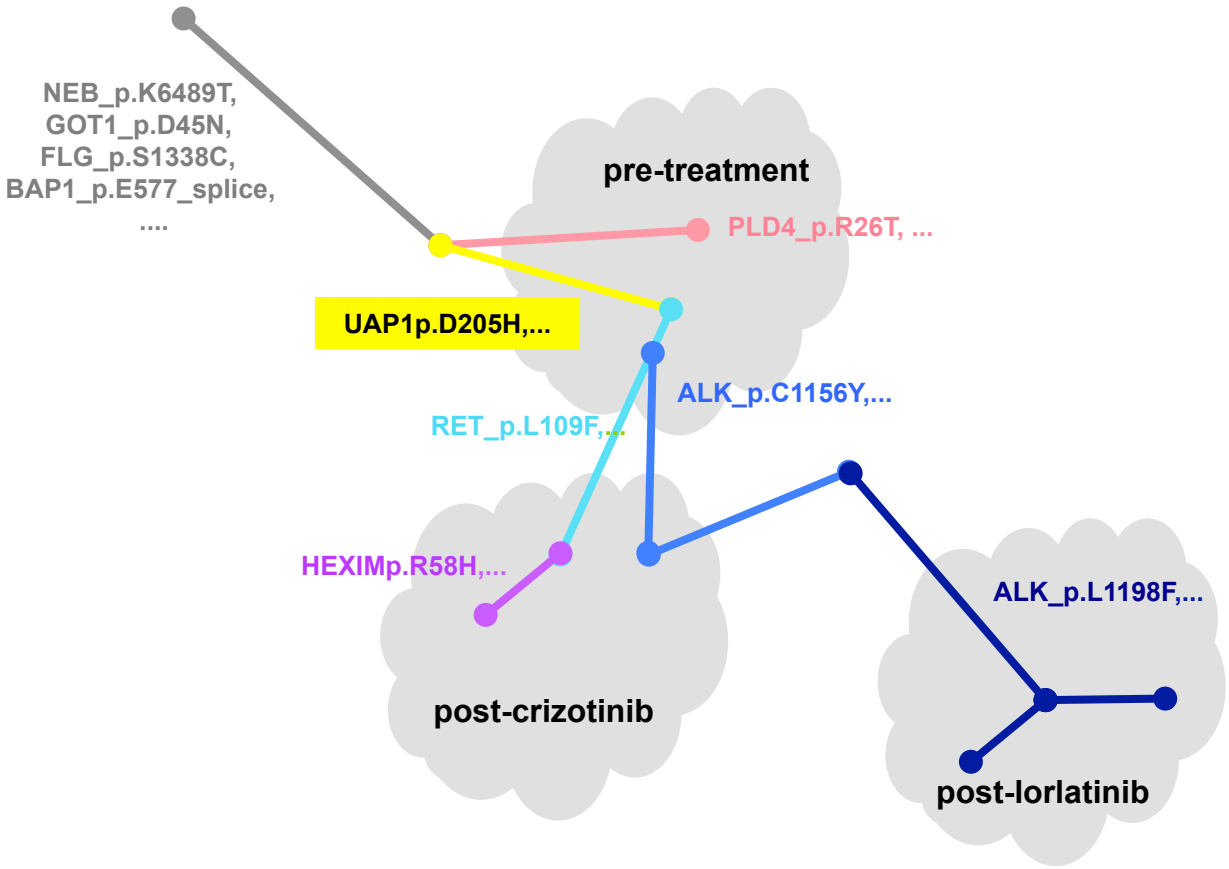

Figure S2. Phylogenetic Relationship of Pre-Treatment and Resistant Samples
This branched diagram or "tree" depicts the clonal evolution of the patient's lung cancer as she became resistant to crizotinib and lorlatinib. Multiple subclones were present in each biopsy, with only the major subclones shown here. The colors of individual subclones correspond to those shown in Figure 1E. Whole exome sequencing and clustering analysis are described in Supplementary Methods.

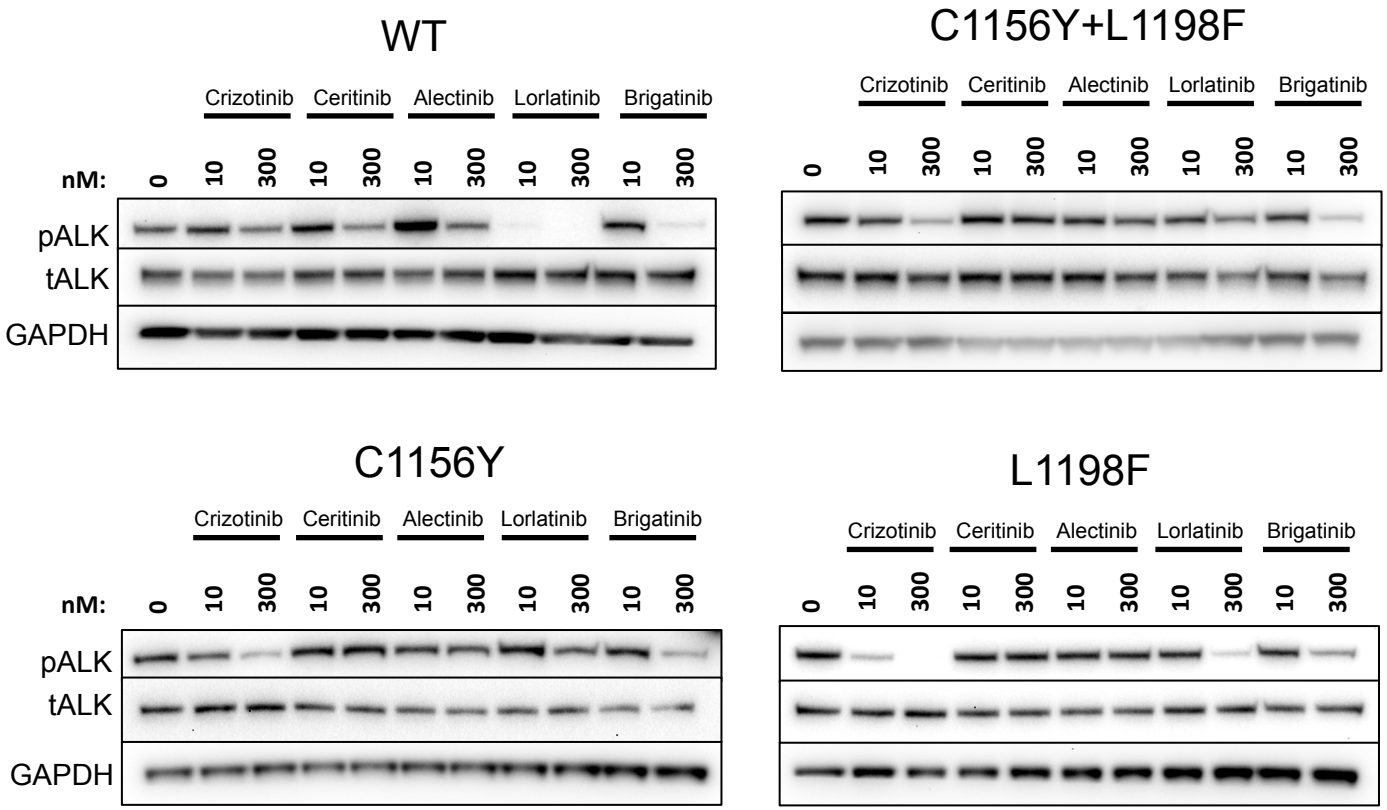

Figure S3. Suppression of ALK C1156Y/L1198F Phosphorylation by Crizotinib
Ba/F3 cells transformed by wildtype or mutant EML4-ALK were treated with the indicated ALK inhibitors for 3 hours. Cell lysates were probed with phospho-ALK (Y1282/1283) and ALK-specific antibodies (Cell Signaling Technology), as well as GAPDH antibody (Millipore). pALK, phosphoALK; tALK, total ALK.

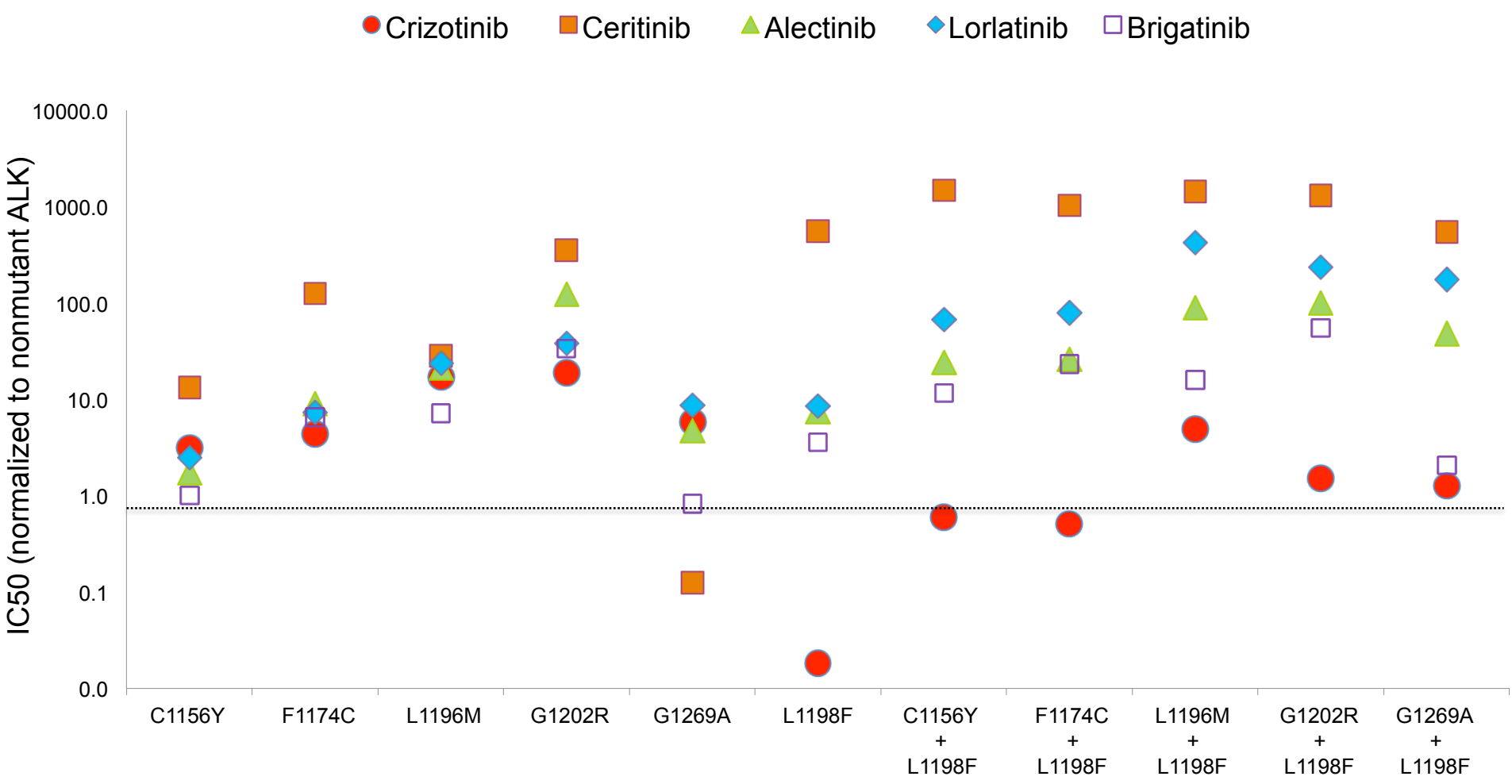

Figure S4. Resensitization of Crizotinib-Resistant ALK Mutants by L1198F
Ba/F3 cells were transformed by wildtype EML4-ALK or EML4-ALK harboring various ALK mutations, as indicated on the x-axis. Ba/F3 lines were treated with different ALK inhibitors for 48 hours. A CellTiter Glo assay (Promega) was then performed to determine relative cell numbers. IC50 values were calculated by concentration-response curve fitting utilizing a four-parameter analytical method. For each drug, the IC50 values for the mutant ALK-expressing Ba/F3 lines have been normalized to that of Ba/F3 cells expressing wildtype EML4-ALK. A normalized IC50 ratio of 1 (dashed line) indicates equivalent sensitivity to wildtype ALK. Ratios less than 1 indicate increased sensitivity, while ratios greater than 1 indicate decreased sensitivity relative to wildtype ALK.

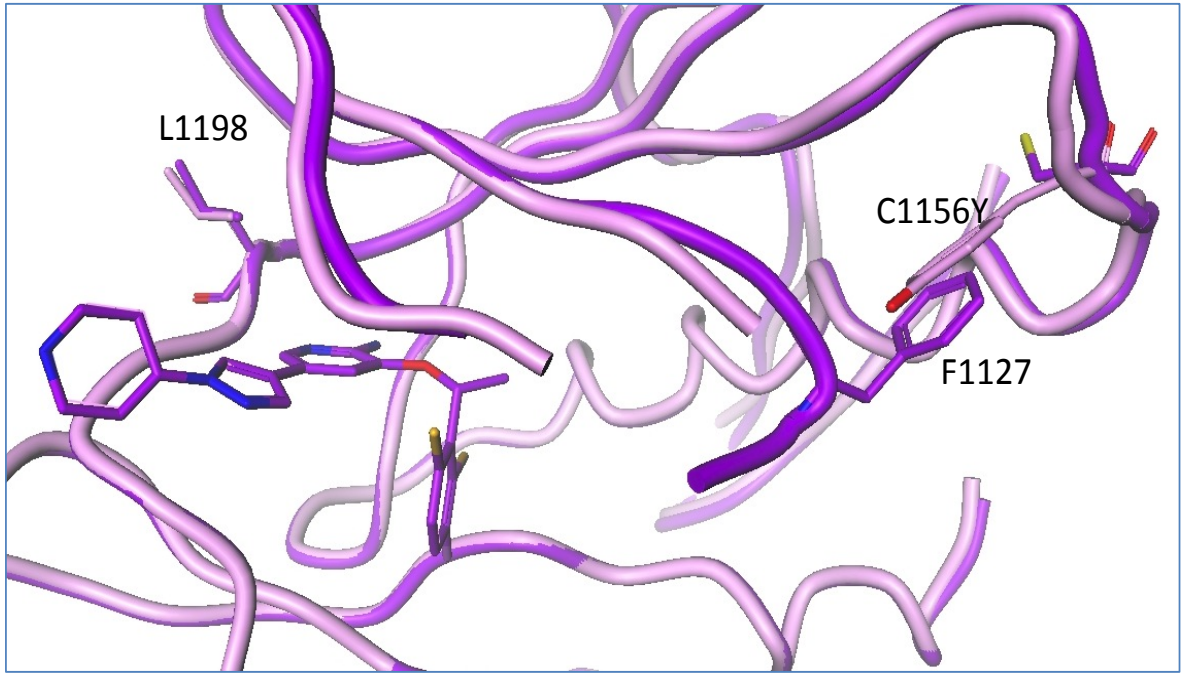

Figure S5. Co-crystal structure of ALK C1156Y with Crizotinib
Shown is an overlay of the co-crystal structures of wildtype ALK (purple) and ALK C1156Y (pink), both bound to crizotinib. The cysteine at position 1156 is remote (13 Å) from the inhibitor binding site, and substitution with tyrosine does not lead to steric interference with the inhibitor. The tyrosine side chain appears to cause the glycine-rich loop to be more dynamic, accelerating substrate on and product off and leading to greater catalytic efficiency, as demonstrated in Table S4. This increase in kinase activity likely underlies C1156Y-mediated resistance to crizotinib. More potent ALK inhibitors, however, may be able to overcome this mutant's increased kinase activity.

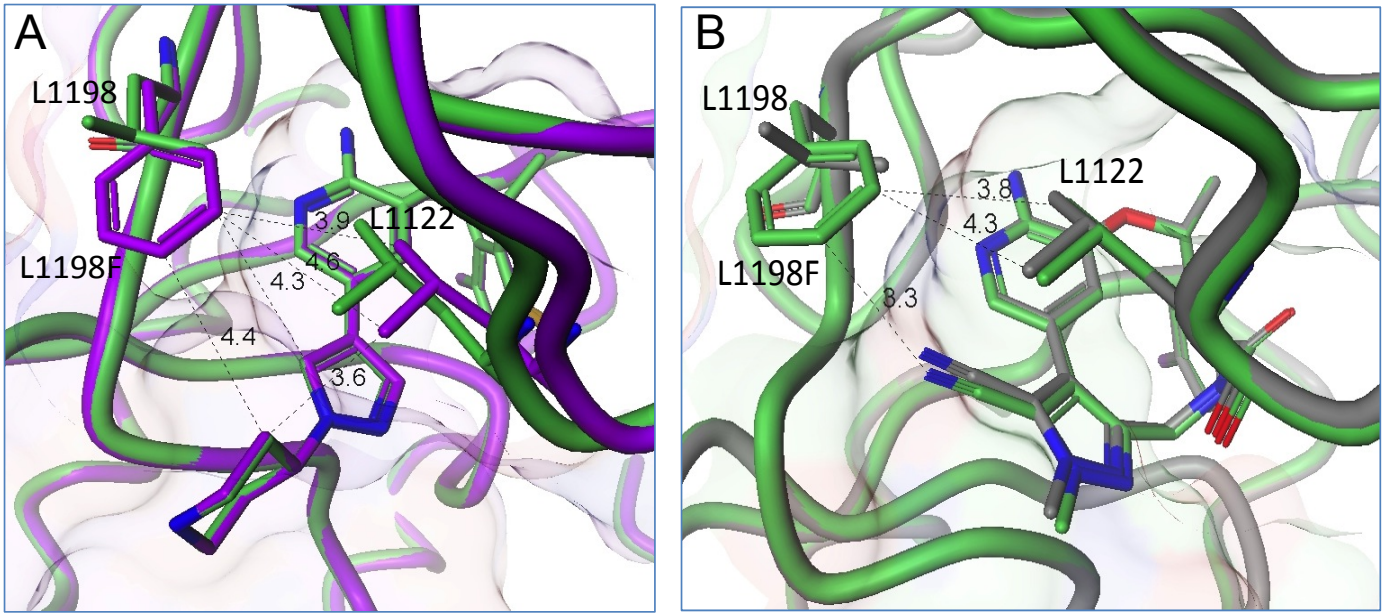

Figure S6. Co-crystal structures of ALK C1156Y and C1156Y/L1198F with Crizotinib or Lorlatinib

(A) Overlay of crizotinib bound to ALK C1156Y (green) and ALK C1156Y/L1198F (purple). In the double mutant, the phenylalanine moves slightly closer to crizotinib. The phenylalanine makes the environment more hydrophobic and contacts a leucine at position 1122 in the G loop above crizotinib. These alterations are energetically more favorable for crizotinib binding. (B) Overlay of lorlatinib bound to ALK C1156Y (gray) and ALK C1156Y/L1198F (green). In order for lorlatinib to bind the double mutant, the nitrile must move 0.4-0.5 Å away relative to its position when the native leucine resides at position 1198. The macrocyclic rigid-body rotation of lorlatinib is energetically unfavorable for binding. Distances are highlighted in angstroms.

Table S1. Cell Survival Assays of Ba/F3 Models Expressing ALK Resistant Mutants[1]

Ba/F3 Model	ALK Inhibitor	IC50, nM	Normalized IC50 to ALK WT
Parental	crizotinib	960.2 ± 120.3	47.3
Parental	lorlatinib	15038.5 ± 4902.5	8573.0
Parental	ceritinib	824.0 ± 140.0	2346.7
Parental	alectinib	880.0 ± 64.2	154.2
Parental	brigatinib	2775.5 ± 443.5	719.8
ALK WT	crizotinib	20.3 ± 4.4	1
ALK WT	lorlatinib	1.8 ± 0.1	1
ALK WT	ceritinib	0.4 ± 0.1	1
ALK WT	alectinib	5.7 ± 1.3	1
ALK WT	brigatinib	3.9 ± 0.4	1
ALK C1156Y	crizotinib	63.7 ± 17.1	3.1
ALK C1156Y	lorlatinib	4.4 ± 0.4	2.5
ALK C1156Y	ceritinib	4.6 ± 2.0	13.2
ALK C1156Y	alectinib	9.8 ± 3.6	1.7
ALK C1156Y	brigatinib	3.9 ± 1.0	1.0
ALK L1198F	crizotinib	0.4 ± 0.2	0.02
ALK L1198F	lorlatinib	14.8 ± 2.7	8.4
ALK L1198F	ceritinib	196.2 ± 13.9	558.9
ALK L1198F	alectinib	42.3 ± 8.7	7.4
ALK L1198F	brigatinib	13.9 ± 2.1	3.6
ALK C1156Y/L1198F	crizotinib	12.3 ± 1.4	0.6
ALK C1156Y/L1198F	lorlatinib	117.0 ± 11.7	66.7
ALK C1156Y/L1198F	ceritinib	524.0 ± 61.3	1492.6
ALK C1156Y/L1198F	alectinib	138.4 ± 31.9	24.2
ALK C1156Y/L1198F	brigatinib	44.6 ± 7.0	11.6

[1]Ba/F3 cell lines expressing the indicated EML4-ALK mutants were treated with different ALK inhibitors for 48 hrs. Cell survival was assayed using a CellTiter-Glo assay. IC50 values were calculated by concentration-response curve fitting utilizing a four-parameter analytical method. Shown in the third column are mean IC50 values ± sem, and in the fourth column IC50 values normalized to that of Ba/F3 cells expressing wildtype EML4-ALK. WT, wildtype.

Table S2. Cell Survival Assays in Ba/F3 Models Expressing Different ALK L1198F Mutants[1]

ALK	Crizotinib	Lorlatinib	Ceritinib	Alectinib	Brigatinib
WT	20.3 ± 4.4	1.8 ± 0.1	0.4 ± 0.1	5.7 ± 1.3	3.9 ± 0.4
L1198F	0.4 ± 0.2	14.8 ± 2.7	196.2 ± 13.9	42.3 ± 8.7	13.9 ± 2.1
C1156Y	63.7 ± 17.1	4.4 ± 0.4	4.63 ± 2.0	9.8 ± 3.6	3.9 ± 1.0
C1156Y/L1198F	12.3 ± 1.4	117.0 ± 11.7	524.0 ± 61.3	138.4 ± 31.9	44.6 ± 7.0
F1174C	88.9 ± 17.9	12.9 ± 2.9	44.0 ± 11.2	52.0 ± 20.9	25.1 ± 8.7
F1174C/L1198F	10.4 ± 3.2	138.6 ± 31.1	364.5 ± 28.2	150.0 ± 34.4	89.2 ± 22.0
L1196M	345.4 ± 35.7	41.7 ± 4.9	9.9 ± 1.8	120.4 ± 40.1	27.7 ± 9.0
L1196M/L1198F	100.2 ± 29.3	735.3 ± 139.4	504.0 ± 183.8	511.9 ± 137.7	61.8 ± 19.7
G1202R	381.6 ± 72.0	67.0 ± 8.3	124.4 ± 21.1	706.6 ± 87.7	129.5 ± 51.6
G1202R/L1198F	30.8 ± 8.1	414.0 ± 92.8	455.6 ± 214.5	569.5 ± 237.1	211.8 ± 45.6
G1269A	117.8 ± 2.0	15.2 ± 0.6	0.04 ± 0.01	27.0 ± 2.3	3.2 ± 0.2
G1269A/L1198F	25.9 ± 5.7	308.6 ± 60.2	192.0 ± 66.2	276.0 ± 58.4	8.1 ± 1.8

[1]Ba/F3 cell lines expressing the indicated EML4-ALK mutants were treated with different ALK inhibitors for 48 hrs. Cell survival was assayed using a CellTiter-Glo assay. IC50 values were calculated by concentration-response curve fitting utilizing a four-parameter analytical method. Shown are mean IC50 values ± sem. WT, wildtype.

Table S3. Inhibition Constants of ALK Inhibitors With Wildtype and Mutant ALK Kinase Domains[1]

ALK Mutation	ALK Inhibitor	Ki, nM	Normalized Ki to ALK WT
WT	crizotinib	1.6 ± 0.1	1
WT	lorlatinib	0.14 ± 0.01	1
WT	ceritinib	0.10 ± 0.01	1
WT	alectinib	0.09 ± 0.01	1
WT	AP26113	0.10 ± 0.01	1
C1156Y	crizotinib	1.3 ± 0.1	0.80
C1156Y	lorlatinib	0.08 ± 0.02	0.57
C1156Y	ceritinib	0.054 ± 0.002	0.54
C1156Y	alectinib	0.12 ± 0.01	1.3
C1156Y	AP26113	0.11 ± 0.01	1.1
L1198F	crizotinib	0.38 ± 0.01	0.24
L1198F	lorlatinib	6.4 ± 0.1	46
L1198F	ceritinib	19.4 ± 0.4	194
L1198F	alectinib	3.3 ± 0.2	37
L1198F	AP26113	4.2 ± 0.2	42
C1156Y/L1198F	crizotinib	0.88 ± 0.02	0.55
C1156Y/L1198F	lorlatinib	8.6 ± 2.9	61
C1156Y/L1198F	ceritinib	5.8 ± 0.2	58
C1156Y/L1198F	alectinib	6.1 ± 0.2	68
C1156Y/L1198F	AP26113	5.8 ± 0.1	58

[1]Ki values were determined using microfluidic mobility shift assay as previously described for ALK and ROS assays (Johnson et al., 2014; Zou at al., 2015). The Ki's are mean values with standard error of the global fits to the Morrison equation for competitive inhibition, using multiple ATP concentrations and experimentally determined apparent ATP Km of 111, 77, 251 and 149 μM for wildtype (WT), C1156Y, L1198F and C1156Y/L1198F mutants, respectively.

Table S4. Kinetic Parameters of Wildtype and Mutant ALK Kinase Domains[1]

ALK variant	k_{cat} (s^{-1})	K_M,ATP (μM)	$K_{M,YFF}$ (μM)	Relative $k_{cat}/K_{M,YFF}$
WT	9.3 ± 0.2	98 ± 7	200 ± 30	1
C1156Y	22.4 ± 1.5	89 ± 9	85 ± 16	5.6
L1198F	3.4 ± 0.1	96 ± 15	193 ± 26	0.4
C1156Y/L1198F	11.3 ± 0.3	59 ± 4	137 ± 18	1.7

[1]Kinetic parameters were determined by a coupled spectrophotometric ATP-regenerating assay using a "YFF" analog of the ALK activation loop peptide, as described in Experimental Procedures. The values are best-fit values derived from the Michaelis-Menten equation for kinetic assays conducted at least in duplicate.

Table S5. Computational Models Comparing Wildtype ALK and ALK L1198F Binding to Crizotinib and Lorlatinib[1]

Ligand	$E_{L1198F} - E_{WT}$ (kcal)	Predicted $K_{d,\ L1198F}$ fold over $K_{d,\ WT}$
crizotinib	-0.82 ± 0.09	0.25
lorlatinib	+1.82 ± 0.08	20

[1]FEP/REST (Schrödinger) modeling of crizotinib and lorlatinib bound to unphosphorylated ALK kinase domain, converting between wildtype and L1198F. Predicted ratios are derived from the energy difference between wildtype and ALK L1198F, with values less than one favoring binding to L1198F and values greater than one favoring binding to wildtype ALK.

Table S6. Energetics of Crizotinib and Lorlatinib Binding to Wildtype and Mutant ALK Kinase Domains[1]

Variant	Compound	K_d (nM)	$K_{d,WT}$ / $K_{d,mut}$	ΔG (kcal mol^{-1})	ΔG_{mut}-ΔG_{WT} (kcal mol^{-1})	ΔH (kcal mol^{-1})	ΔH_{mut}-ΔH_{WT} (kcal mol^{-1})
WT	crizotinib	5.0 ± 0.7	1	-11.1	0	-13.4 ± 1.4	0
	lorlatinib	0.38 ± 0.07	1	-12.7	0	-16.0 ± 0.5	0
C1156Y	crizotinib	2.4 ± 0.8	0.48	-11.6	-0.5	-13.1 ± 1.0	+0.3
	lorlatinib	ND	ND	ND	ND	ND	ND
L1198F	crizotinib	1.4 ± 1.2	0.28	-11.9	-0.8	-13.8 ± 1.8	-0.4
	lorlatinib	7.7 ± 2.8	20	-10.9	+1.8	-14.0 ± 2.2	+2.0
C1156Y/ L1198F	crizotinib	2.0 ± 0.9	0.40	-11.7	-0.6	-15.1 ± 1.1	-1.7
	lorlatinib	7.9 ± 1.8	21	-10.9	+1.8	-12.3 ± 0.3	+3.7

[1]Energetic parameters were determined by isothermal titration calorimetry at 20 ^{o}C by direct monitoring of the enthalpy change (ΔH), for compound binding to the wildtype and mutant ALK kinase domains.

REFERENCES

1. Li H, Durbin R. Fast and accurate short read alignment with Burrows-Wheeler transform. Bioinformatics 2009;25:1754-60.
2. Cibulskis K, Lawrence MS, Carter SL, et al. Sensitive detection of somatic point mutations in impure and heterogeneous cancer samples. Nature biotechnology 2013;31:213-9.
3. Fisher S, Barry A, Abreu J, et al. A scalable, fully automated process for construction of sequence-ready human exome targeted capture libraries. Genome biology 2011;12:R1.
4. Gnirke A, Melnikov A, Maguire J, et al. Solution hybrid selection with ultra-long oligonucleotides for massively parallel targeted sequencing. Nature biotechnology 2009;27:182-9.
5. Chapman MA, Lawrence MS, Keats JJ, et al. Initial genome sequencing and analysis of multiple myeloma. Nature 2011;471:467-72.
6. Lohr JG, Stojanov P, Lawrence MS, et al. Discovery and prioritization of somatic mutations in diffuse large B-cell lymphoma (DLBCL) by whole-exome sequencing. Proceedings of the National Academy of Sciences of the United States of America 2012;109:3879-84.
7. Ramos AH, Lichtenstein L, Gupta M, et al. Oncotator: cancer variant annotation tool. Human mutation 2015;36:E2423-9.
8. Carter SL, Cibulskis K, Helman E, et al. Absolute quantification of somatic DNA alterations in human cancer. Nature biotechnology 2012;30:413-21.
9. Landau DA, Carter SL, Stojanov P, et al. Evolution and impact of subclonal mutations in chronic lymphocytic leukemia. Cell 2013;152:714-26.
10. Escobar MD, West M. Bayesian Density Estimation and Inference Using Mixtures. J Amer Statistical Assoc 1995;90:577-88.
11. Lohr JG, Stojanov P, Carter SL, et al. Widespread genetic heterogeneity in multiple myeloma: implications for targeted therapy. Cancer cell 2014;25:91-101.
12. Friboulet L, Li N, Katayama R, et al. The ALK inhibitor ceritinib overcomes crizotinib resistance in non-small cell lung cancer. Cancer discovery 2014;4:662-73.
13. Johnson TW, Richardson PF, Bailey S, et al. Discovery of (10R)-7-amino-12-fluoro-2,10,16-trimethyl-15-oxo-10,15,16,17-tetrahydro-2H-8,4-(m etheno)pyrazolo[4,3-h][2,5,11]-benzoxadiazacyclotetradecine-3-carbonitrile (PF-06463922), a macrocyclic inhibitor of anaplastic lymphoma kinase (ALK) and c-ros oncogene 1 (ROS1) with preclinical brain exposure and broad-spectrum potency against ALK-resistant mutations. Journal of medicinal chemistry 2014;57:4720-44.
14. Zou HY, Li Q, Engstrom LD, et al. PF-06463922 is a potent and selective next-generation ROS1/ALK inhibitor capable of blocking crizotinib-resistant ROS1 mutations. Proceedings of the National Academy of Sciences of the United States of America 2015;112:3493-8.
15. Timofeevski SL, McTigue MA, Ryan K, et al. Enzymatic characterization of c-Met receptor tyrosine kinase oncogenic mutants and kinetic studies with aminopyridine and triazolopyrazine inhibitors. Biochemistry 2009;48:5339-49.
16. Donella-Deana A, Marin O, Cesaro L, et al. Unique substrate specificity of anaplastic lymphoma kinase (ALK): development of phosphoacceptor peptides for the assay of ALK activity. Biochemistry 2005;44:8533-42.